

11<sup>th</sup> International  
Conference on Fracture  
Turin (Italy) - March 20-25, 2005

ATOMIC SCALE FRICTION AND ITS CONNECTIONS TO  
FRACTURE

R.W. Carpick

Department of Engineering Physics, University of Wisconsin-Madison, Madison, WI 53706 USA

ABSTRACT

The contact between an atomic force microscope tip and a sample surface can form an ideal single asperity of nanometer dimensions, where the interaction forces can be measured with sub-nanoNewton force resolution. Studies of contact, adhesion and friction for these nano-asperities have been carried out for a variety of tips and single crystal sample surfaces, both in ambient conditions and ultrahigh vacuum. The major result is the observation of proportionality between friction and true contact area for a variety of systems, and impressive agreement with continuum mechanics models even at the nanometer scale, although several features unique to the nanoscale are also observed. The relevant continuum models can in fact be understood in the framework of a scale-dependent fracture mechanics model. We will discuss how adhesive models of contact, which can be derived from fracture mechanics approaches, are used to determine what we propose are the fundamental tribological parameters of nanoscale interfaces: the interfacial shear strength, and the work of adhesion.

1 INTRODUCTION

As devices shrink in size, the increased surface-to-volume ratio of the components ensures that interfacial forces such as friction and adhesion play dominant roles. This fact is painfully appreciated by the designers of microelectromechanical systems (MEMS) who often observe catastrophic failure of MEMS due to adhesion, friction and wear. Understanding these interfacial forces may allow such problems to be remedied, and furthermore, the relative strength of these forces could potentially be exploited for specific micro- and nano-scale device applications.

There is currently no fundamental theory to explain or predict friction. Macroscopically, the friction force ( $F_f$ ) is usually linearly proportional to the normal force or load ( $L$ ):

$$F_f = \mu \cdot L \quad (1)$$

which defines the friction coefficient  $\mu$ . Eqn. (1) is referred to as Amontons' Law. Macroscopic studies are complicated by the effects of roughness, wear, third-bodies and tribochemistry.

The atomic force microscope (AFM) is an important tool with which to study contact and friction in a fundamental way [1]. A tip, with typically 10-100 nm radius of curvature, is attached to a compliant cantilever spring. At low applied loads, the tip can form a nanometer-scale single contact point (an "asperity") with a variety of sample surfaces, thus providing a well-defined interface. The cantilever deflections are recorded using, most commonly, a reflected optical beam. These deflections are converted to forces by using Hooke's Law. In principle, the normal and lateral forces can be measured with sub-nanoNewton precision, with sub-Ångstrom displacement precision. This tip is rastered over the surface using piezoelectric scanning tubes.

2 EXPERIMENT

The experiments described here were conducted using either an ultrahigh vacuum atomic force microscope which is described elsewhere [3], or a Digital Instruments Multimode AFM using a Nanoscope IV controller. Experiments were performed at room temperature. Microfabricated cantilevers from commercial vendors were used. Scanning electron microscopy measurements of

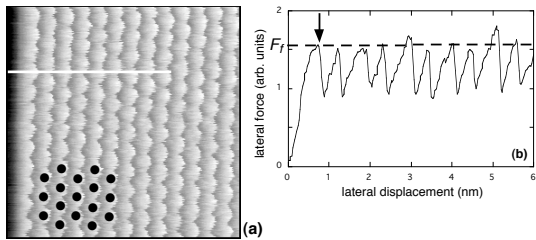


Figure 1. (a)  $7.5 \times 7.5 \text{ nm}^2$  lateral force image of the mica surface. The fast scan direction is from left to right. The black dots represent the repeat units of the mica lattice, whose periodicity coincides with the lateral forces. (b) Line trace of the section indicated in (a). The lateral force exhibits “stick-slip” behaviour, where the lateral force builds up to some well-defined maximum value, and then quickly relaxes (first arrow) by one unit cell.

diamond-like carbon (DLC) thin film sample. DLC films were deposited on silicon wafers using the non-line-of-sight plasma source ion deposition process [7].

### 3 RESULTS

#### 3.1 Atomic-lattice stick-slip

Frequently, when an AFM tip is placed in contact with a crystalline sample and scanned across it to generate a force map, atomic-scale periodicity is observed (Figure 1(a)) [8]. Lateral and normal forces are observed to vary with the periodicity of the sample’s lattice. This behavior has been observed for a wide variety of tips and samples, and a wide range of experimental conditions (liquid, ambient, controlled atmosphere, vacuum) [1]. When examined in detail (Figure 1(b)), this behavior is seen to result from discontinuous motion of the tip along the surface. As the lever is continuously rastered across the sample, the tip traces out the sample’s lattice through a regular series of stick-slip events [8]. The observed slip can be thought of as a fracture event: the interface has ruptured, and slip by one Burger’s vector (the lattice constant) has occurred.

As seen in Figure 1(b), there is a reproducible lateral force at which the slip occurs. We are interested in understanding what determines this atomic-scale static friction force,  $F_f$ . To do this, we measure the average value of this friction force at a given load, change the load slightly, then measure the friction again, and so on. Typically we measure half of the difference between the average friction force obtained scanning left-to-right and right-to-left, which greatly reduces signal offsets due to coupling of bending modes and optical misalignment. Atomic-scale stick-slip was observed for both the Pt/mica experiments. It was not observed for the SiN/DLC experiment, which is not surprising since both the DLC and the SiN are amorphous; there is no periodicity.

#### 3.2 Pt/mica interface

Figure 2 shows the variation of friction (circles) with load for the Pt/mica interface. Friction is a non-linear function of load in contradiction with the macroscopic law of Amontons, Eqn. (1). A substantial negative load (the *pull-off force*) must be applied to separate the tip and sample. The data is well-fit by the Johnson-Kendall-Roberts (JKR) [9] model for the contact area between a paraboloidal tip and a flat plane. The JKR model balances elastic strain energy with adhesive interfacial energy to determine the contact area. The end result is a simple, analytic equation:

cantilever dimensions were combined with continuum elasticity theory calculations to estimate the normal force spring constants. Lateral forces were calibrated with respect to the normal forces using the “wedge calibration technique” [2]. The tip geometry was experimentally determined using “inverse imaging” [4]. Unless otherwise noted, the tip was determined to be paraboloidal.

Two sets of interfaces are discussed here:

(1) A platinum-coated tip and a muscovite mica(0001) sample in UHV [5,6]. The 100 nm Pt coating was deposited by sputtering onto a plasma-cleaned silicon nitride cantilever. Muscovite mica was cleaved inside the vacuum chamber prior to the experiment, producing large step-free regions.

(2) A silicon nitride tip (SiN) and a

$$A = \sqrt{\frac{3R}{4E^*}} \left( L + 3\sqrt{\gamma}R + \sqrt{6\sqrt{\gamma}RL + (3\sqrt{\gamma}R)^2} \right)^{2/3} \quad (2)$$

where  $A$  is the contact area,  $R$  is the tip radius,  $\gamma$  is the work of adhesion (also known as the Dupré energy of adhesion).  $E^*$  is the reduced Young's modulus of the tip and sample materials, given by  $E^* = \left( (1-\nu_1^2)/E_1 + (1-\nu_2^2)/E_2 \right)^{-1}$  where  $E_1$ ,  $E_2$  are the Young's moduli of the tip and sample respectively, and  $\nu_1$ ,  $\nu_2$  the respective Poisson's ratios. The JKR relation requires that the tip is paraboloidal. Inverse imaging, described above, verifies that the tip is paraboloidal with a curvature radius of  $\sim 140$  nm.

Since contact area varies with load in almost exact proportion to friction, we postulate that:

$$F_f = \gamma \cdot A \quad (4)$$

where  $\gamma$  is the interfacial shear strength. Eqn. (4) thus represents the essential relation governing friction for an elastic single asperity. Furthermore, the pull-off force can be used to determine the work of adhesion from the following equation:

$$\gamma = \frac{2L_c}{3\sqrt{R}} \quad (5)$$

We further tested the validity of the JKR approach by deliberately altering the tip shape through application of an extremely high load while sliding. A blunt, flat tip was produced in this fashion, as verified by inverse imaging. The JKR prediction for contact area will obviously depend upon the tip geometry. We confirmed that the observed friction-load data was well fit by a modified JKR model derived using an appropriately flat tip profile [5].

By using bulk values for the elastic constants ( $E_{mica} = 56.5$  GPa,  $\nu_{mica} = 0.098$  [10],  $E_{Pt} = 177$  GPa,  $\nu_{Pt} = 0.39$  [11]), we can solve for the contact radius at zero load, listed in Table 1. We see that indeed the contact is of nanometer dimensions. Smaller contacts can be formed with smaller tips and less strongly adhering materials. The JKR analysis also allows us to determine both the interfacial energy ( $\gamma$ ) and the shear strength ( $\tau$ ) for this interface (Table 1). The values quoted are for the maximum shear strength and adhesion energy observed for this system; a gradual decrease of both of these ensued due to contact-induced changes in the tip chemistry, as described elsewhere [6]. The adhesion energy (derived from the pull-off force) is relatively strong, surpassing the van der Waals' energy by an order of magnitude. Likewise, the shear strength is

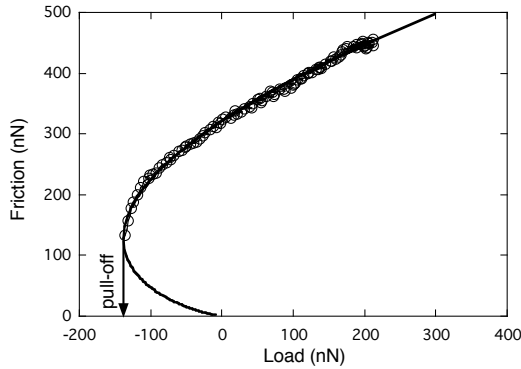


Figure 2. Friction (circles) vs. load for a Pt-coated tip in contact with mica in UHV. The tip is initially loaded to  $\sim 210$  nN, then the load is decreased. At  $-140$  nN, the tip pulls out of contact with the sample. The solid line is the JKR prediction for the contact area vs. load.

extremely large. The theoretical prediction for the shear strength of a crystalline material in the absence of dislocations is given by  $\sim G/30$  [12] where  $G$  is the shear modulus. We define an effective interfacial contact modulus in shear as  $G_{eff} = 2G_{mica}G_{Pt}/(G_{mica} + G_{Pt}) \approx 22.3$  GPa. This gives, for Pt/mica,  $\tau \approx G_{eff}/25$ . The shear strength of this system is thus comparable to Frenkel's model for the "ideal" material shear strength [13] whereby the shear strength is approximately 1/30th of the shear modulus for a crystal in the absence of dislocations.

### 3.3 SiN/DLC interface

Figure 4 shows the variation of friction with load for a DLC film in an environment of  $<5$  and 60% RH measured with a SiN tip. A measurement was acquired at 5% RH, then a series of subsequent measurements (not shown)

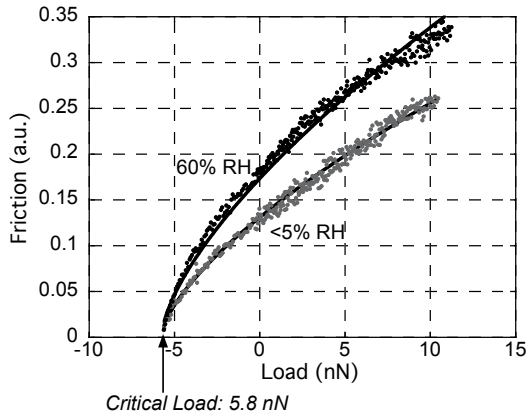


Figure 3. Friction vs. load at <5% (gray) and 60% (black) RH. Solid lines: DMT fits to the data.

were acquired at progressively increasing RH up to 60%, then the RH was lowered again back to <5%. The data overlap extremely closely at each humidity. Friction is clearly higher at 60% RH, but the pull-off force is identical. For all friction vs. load measurements, friction monotonically increases with humidity, but no variation of the pull-off force is observed.

The data are in excellent agreement with Eqn. (4), but this time  $A$  is not described by the JKR model, but rather by the Derjaguin-Müller-Toporov (DMT) model (Figure 4, solid lines) [14]. This theory is similar to the Hertz theory for non-adhesive contacts [15], except that interfacial adhesion gives an offset to the area-load curve so that the surfaces separate at a negative force. The DMT model predicts that

the contact area  $A$  should vary with load  $L$  as follows:

$$A = \sqrt{\frac{3R}{4E^*}} \cdot (L + L_c)^{3/2} \quad (6)$$

where,  $L_c$  is the critical load or pull-off force. The shear strength is plotted changes by a factor of 1.4 from <5% to 60% RH. The DMT relation gives the work of adhesion  $\gamma$  of the interface:

$$\gamma = \frac{L_c}{2\sqrt{R}}, \quad (7)$$

which is similar to Eqn. (5), but with a different numerical factor. The average work of adhesion for all the measurements here is  $0.0547 \pm 0.0004 \text{ J/m}^2$ .

According to classical meniscus theory applied to our conditions, the pull-off force ought vary substantially with RH [16]. The lack of any change indicates that classical meniscus theory fails, in accordance with other AFM measurements [17-19]. While the interpretation of the structure and kinetics of water at this scale is speculative, a minimum amount may be required to form a meniscus, and that is not possible on the hydrophobic DLC film. The presence of water molecules nonetheless has a significant effect on friction. There is no experimental technique which can discern the chemistry and structure of water (or any other species) confined at this nanoscale interface *in-situ*. A study using a technique such as molecular dynamics is necessary to understand this behavior in more detail.

#### 4 CONNECTIONS TO FRACTURE MECHANICS

In the previous two examples, the friction force is proportional to the true area of contact, with the constant of proportionality being an interfacial shear strength that is independent of pressure for the regime studied (Eqn. (4)). In both cases, the contact remains in the elastic regime. Either the JKR or DMT models of adhesive elastic contact provide excellent fits to the data. A number of other studies have also demonstrated agreement with Eqn. (4) [1,5,6,20-31], and in some cases the shear strength does exhibit a pressure dependence [32,33]. However, the JKR and DMT models neglect the application of any tangential load. Furthermore, cases intermediate to the JKR and DMT models have not yet been addressed. To deal with these complications, fracture mechanics can be used.

The JKR model, for example, can be derived using fracture mechanics [34,35]. The contact is viewed as an external circular crack in an infinite medium. The contact edge represents the crack front. Loading and unloading is viewed as propagating this crack (advancing or receding) in mode I. Adhesion is thus represented by attractive forces in a cohesive zone, and the load is represented

as the applied external separation force. Griffith's concept of brittle fracture is used to balance strain energy and interfacial energy to solve for the contact area as a function of load, as summarized elsewhere [34].

Since it is based on the Griffith concept, the JKR model assumes that the interfacial attraction has zero spatial range; *i.e.* the system gains energy only when the materials are in direct contact. This approach is reasonable only for relatively compliant, strongly adhering materials exhibiting short-range attraction. Finite range forces have been modeled by others [36,37], with the extreme opposite limit for stiff, weakly adhering materials with long-range forces described by the DMT theory [14]. Intermediate cases are treated by Maugis [37] using a Dugdale crack model. Again, using a mode I fracture mechanics approach, this time with a constant adhesive stress acting over a *finite* distance, Maugis provides an analytic solution that predicts the contact area for the JKR and DMT limits, and for cases in between. Maugis' equations are relatively complicated; a simplified form of the solution has been derived which facilitates fitting this model to experimental data [38]. In any event, for these cases, the contact area varies with load in a significantly different fashion compared with the JKR solution.

These models assume only normal loading, thus neglecting effects that the substantial applied lateral force has upon the contact area. Johnson [34] has combined the Dugdale model of Maugis with interacting mode I, II and III fracture mechanics. This theory thus includes the influence of the lateral force upon the contact area, and allows the interaction forces to have a finite range. Using this finite range mixed-mode fracture approach, Johnson predicts that the contact area can be reduced appreciably by partial slip at the contact edge which is induced by the applied lateral force. Reference [34] contains a comparison to the same data shown in Figure 2. According to this model, the shape of the area-load relation for this particular set of data still resembles the JKR curve, but with different (smaller) absolute values. The model also predicts that the lateral force causes pull-off to occur at a smaller load compared to the direct pull-off force (measured without sliding). This model can be tested with AFM by comparing the direct and sliding pull-off forces. A statistical analysis was conducted for the Pt/mica system, revealing an average reduction of the pull-off force by a factor of 0.89 due to sliding. Using this result, the data presented in Figure 2 can be fit by this modified theory, resulting in an increase of the shear strength by about 20% compared with the JKR fit. While the observed pull-off reduction supports Johnson's model, it is not a direct verification that the contact area itself changes due to sliding.

The high shear strength observed for the Pt/mica interface remains to be fully explained. It is consistent with large shear strengths reported in other experiments [27,28,39]. Recent modeling by Hurtado and Kim [13,40] using dislocation mechanics suggests that below a critical contact size (in the nm range), strongly adhered contacts should exhibit such ideal shear strengths. The strong attractive forces may create a substantial degree of commensurability of the interfacial atoms, thus producing an interface that is resistant to shear, as in a crystalline material. At this scale, according to the theory, the contact is too small to allow the nucleation of even a single dislocation at the contact edge. Dislocation nucleation is predicted to reduce the shear strength substantially at larger scales. Experiments that test this model more thoroughly are desirable.

## 5 CONCLUSIONS

Single-asperity friction measurements at the nano-scale consistently reveal that the friction force is proportional to the true interfacial area of contact, frequently resulting in a non-linear dependence of friction upon load. Fracture mechanics provides a useful formalism for describing the complex relationship between contact area and load for these adhesive contacts which are also subject to significant tangential loads. While further work is required to fully verify these models, these advances have shed new light onto the mechanics of nano-scale friction, and this insight can now be applied to the more challenging study of real, multi-asperity contacting interfaces such as those present in micromachine devices or macroscopic systems.

## 6 REFERENCES

- [1] Carpick, R.W. and Salmeron, M., *Chem. Rev.* **97**, (1997) p. 1163.
- [2] Ogletree, D.F., Carpick, R.W., and Salmeron, M., *Rev. Sci. Instrum.* **67**, (1996) p. 3298.
- [3] Dai, Q., Vollmer, R., Carpick, R.W., Ogletree, D.F., and Salmeron, M., *Rev. Sci. Instrum.* **66**, (1995) p. 5266.
- [4] Villarrubia, J.S., *Surf. Sci.* **321**, (1994) p. 287.
- [5] Carpick, R.W., Agraït, N., Ogletree, D.F., and Salmeron, M., *J. Vac. Sci. Technol. B* **14**, (1996) p. 1289.
- [6] Carpick, R.W., Agraït, N., Ogletree, D.F., and Salmeron, M., *Langmuir* **12**, (1996) p. 3334.
- [7] Malik, S.M., Fetherston, R.P., and Conrad, J.R., *J. Vac. Sci. Technol. A* **15**, (1997) p. 2875.
- [8] Morita, S., Fujisawa, S., and Sugawara, Y., *Surf. Sci. Rep.* **23**, (1996) p. 3.
- [9] Johnson, K.L., Kendall, K., and Roberts, A.D., *Proc. Roy. Soc. London A* **324**, (1971) p. 301.
- [10] McNeil, L.E. and Grimsditch, M., *J. Phys.: Condens. Matter* **5**, (1992) p. 1681.
- [11] *Metals handbook* (American Society for Metals, Metals Park, Ohio, 1990).
- [12] Cottrell, A.H., *Introduction to the modern theory of metals* (Institute of Metals, London Brookfield, VT, USA, 1988).
- [13] Hurtado, J.A. and Kim, K.-S., *Proc. Roy. Soc. London A* **455**, (1999) p. 3363.
- [14] Derjaguin, B.V., Muller, V.M., and Toporov, Y.P., *J. Colloid Interface Sci.* **53**, (1975) p. 314.
- [15] Hertz, H., *J. Reine Angew. Math.* **92**, (1881) p. 156.
- [16] Carpick, R.W. and Batteas, J.D., in *Handbook of nanotechnology*, edited by B. Bhushan (Springer-Verlag, New York, 2004).
- [17] Xu, L., Lio, A., Hu, J., Ogletree, D.F., and Salmeron, M., *J. Phys. Chem. B* **102**, (1998) p. 540.
- [18] Xiao, X. and Linmao, Q., *Langmuir* **16**, (2000) p. 8153.
- [19] He, M., Blum, A.S., Aston, D.E., Buenviaje, C., Overney, R.M., and Luginbuhl, R., *J. Chem. Phys.* **114**, (2001) p. 1355.
- [20] Burns, A.R., Houston, J.E., Carpick, R.W., and Michalske, T.A., *Langmuir* **15**, (1999) p. 2922.
- [21] Burns, A.R., Houston, J.E., Carpick, R.W., and Michalske, T.A., *Phys. Rev. Lett.* **82**, (1999) p. 1181.
- [22] Carpick, R.W., Enachescu, M., Ogletree, D.F., and Salmeron, M., in *Fracture and ductile vs. Brittle behavior - theory, modeling and experiment.*, edited by G. Beltz, K.-S. Kim and R.L. Selinger (Mater. Res. Soc., Warrendale, PA, USA, 1999), p. 93.
- [23] Enachescu, M., van den Oetelaar, R.J.A., Carpick, R.W., Ogletree, D.F., Flipse, C.F.J., and Salmeron, M., *Phys. Rev. Lett.* **81**, (1998) p. 1877.
- [24] Enachescu, M., Oetelaar, R.J.A.v.d., Carpick, R.W., Ogletree, D.F., Flipse, C.F.J., and Salmeron, M., *Trib. Lett.* **7**, (1999) p. 73.
- [25] Carpick, R.W., Ogletree, D.F., and Salmeron, M., *Appl. Phys. Lett.* **70**, (1997) p. 1548.
- [26] Lüthi, R., Meyer, E., Bammerlin, M., Howald, L., Haefke, H., Lehmann, T., Loppacher, C., Güntherodt, H.-J., Gyalog, T., and Thomas, H., *J. Vac. Sci. Technol. B* **14**, (1996) p. 1280.
- [27] Lantz, M.A., O'Shea, S.J., Hoole, A.C.F., and Welland, M.E., *Appl. Phys. Lett.* **70**, (1997) p. 970.
- [28] Lantz, M.A., O'Shea, S.J., Welland, M.E., and Johnson, K.L., *Phys. Rev. B* **55**, (1997) p. 10776.
- [29] Pietrement, O. and Troyon, M., *Langmuir* **17**, (2001) p. 6540.
- [30] Pietrement, O. and Troyon, M., *Surf. Sci.* **490**, (2001) p. L592.
- [31] Wei, Z., Wang, C., and Bai, C., *Langmuir* **17**, (2001) p. 3945.
- [32] Briscoe, B.J. and Evans, D.C.B., *Proc. Roy. Soc. London A* **380**, (1982) p. 389.
- [33] Singer, I.L., Bolster, R.N., Wegand, J., Fayeulle, S., and Stupp, B.C., *Appl. Phys. Lett.* **57**, (1990) p. 995.
- [34] Johnson, K.L., *Proc. Roy. Soc. London A* **453**, (1997) p. 163.
- [35] Maugis, D. and Barquins, M., *J. Phys. D. (Appl. Phys.)* **11**, (1978) p. 1989.
- [36] Greenwood, J.A., *Proc. Roy. Soc. London A* **453**, (1997) p. 1277.
- [37] Maugis, D., *J. Colloid Interface Sci.* **150**, (1992) p. 243.
- [38] Carpick, R.W., Ogletree, D.F., and Salmeron, M., *J. Colloid Interface Sci.* **211**, (1999) p. 395.
- [39] Schwarz, U.D., Allers, W., Gensterblum, G., and Wiesendanger, R., *Phys. Rev. B* **52**, (1995) p. 14976.
- [40] Hurtado, J.A. and Kim, K.-S., *Proc. Roy. Soc. London A* **455**, (1999) p. 3385.